Analytical model and figures of merit for filtered Microwave photonic links

Ivana Gasulla* **and José Capmany**

ITEAM Research Institute, Universidad Politécnica de Valencia, Camino de Vera s/n, 46022 Valencia, Spain
**ivgames@iteam.upv.es*

Abstract: The concept of filtered Microwave Photonic Links is proposed in order to provide the most general and versatile description of complex analog photonic systems. We develop a field propagation model where a global optical filter, characterized by its optical transfer function, embraces all the intermediate optical components in a linear link. We assume a non-monochromatic light source characterized by an arbitrary spectral distribution which has a finite linewidth spectrum and consider both intensity modulation and phase modulation with balanced and single detection. Expressions leading to the computation of the main figures of merit concerning the link gain, noise and intermodulation distortion are provided which, to our knowledge, are not available in the literature. The usefulness of this derivation resides in the capability to directly provide performance criteria results for complex links just by substituting in the overall closed-form formulas the numerical or measured optical transfer function characterizing the link. This theory is presented thus as a potential tool for a wide range of relevant microwave photonic application cases which is extendable to multiport radio over fiber systems.

OCIS codes: (060.2330) Fiber optics communications; (060.2360) Fiber optics links and subsystems; (060.5625) Radio frequency photonics; (070.1170) Analog optical signal processing.

References and links

1. A. J. Seeds and K. J. Williams, "Microwave photonics," J. Lightwave Technol. **24**(12), 4628–4641 (2006).
2. J. Capmany and D. Novak, "Microwave Photonics combines two worlds," Nat. Photonics **1**(6), 319–330 (2007).
3. C. H. Cox III, *Analog Photonic Links: Theory and Practice* (Cambridge University Press, Cambridge, U.K., 2004).
4. V. J. Urick, M. S. Rogge, F. Bucholtz, and K. J. Williams, "The performance of analog photonic links employing highly-compressed erbium-doped fiber amplifiers," IEEE Trans. Microw. Theory Tech. **54**(7), 3141–3145 (2006).
5. V. J. Urick, F. Bucholtz, P. S. Devgan, J. D. McKinney, and K. J. Williams, "Phase Modulation With Interferometric Detection as an Alternative to Intensity Modulation With Direct Detection for Analog-Photonic Links," IEEE Trans. Microw. Theory Tech. **55**(9), 1978–1985 (2007).
6. J. M. Wyrwas and M. C. Wu"Dynamic Range of Frequency Modulated Direct-Detection Analog Fiber Optic Links," J. Lightwave Technol. **27**(24), 5552–5562 (2009).
7. T. E. Darcie and P. F. Driessen, "Class-AB techniques for high-dynamic-range microwave-photonic links," IEEE Photon. Technol. Lett. **18**(8), 929–931 (2006).
8. J. D. McKinney and K. J. Williams, "Sampled analog optical links," IEEE Trans. Microw. Theory Tech. **57**(8), 2093–2099 (2009).
9. V. J. Urick, M. Godinez, P. S. Devgan, J. D. McKinney, and F. Bucholtz, "Analysis of an analog fiber-optic link employing a low-biased mach-zehnder modulator followed by an erbium-doped fiber amplifier," J. Lightwave Technol. **27**(12), 2013–2019 (2009).
10. T. E. Darcie, J. Zhang, P. F. Driessen, and J.-J. Eun, "Class-B Microwave-Photonic Link Using Optical Frequency Modulation and Linear Frequency Discriminators," J. Lightwave Technol. **25**(1), 157–164 (2007).
11. H. Chi, X. Zou, and J. Yao, "Analytical Models for Phase-Modulation-Based Microwave Photonic Systems With Phase Modulation to Intensity Modulation Conversion Using a Dispersive Device," J. Lightwave Technol. **27**(5), 511–521 (2009).

#151909 - $15.00 USD Received 27 Jul 2011; revised 28 Aug 2011; accepted 31 Aug 2011; published 23 Sep 2011

12. D. Marpaung, C. Roeloffzen, A. Leinse, and M. Hoekman, "A photonic chip based frequency discriminator for a high performance microwave photonic link," Opt. Express **18**(26), 27359–27370 (2010).
13. B. Moslehi, "Analysis of optical phase noise in fiber-optic systems employing a laser source with arbitrary coherence time," J. Lightwave Technol. **4**(9), 1334–1351 (1986).
14. D. Marcuse, "Pulse distortion in single-mode fibers," Appl. Opt. **19**(10), 1653–1660 (1980).
15. F. Devaux, Y. Sorel, and J. F. Kerdiles, "Simple measurement of fiber dispersion and of chirp parameter of intensity modulated light emitter," J. Lightwave Technol. **11**(12), 1937–1940 (1993).
16. G. Yabre, "Comprehensive Theory of Dispersion in Graded-Index Optical Fibers," J. Lightwave Technol. **18**(2), 166–177 (2000).
17. I. Gasulla and J. Capmany, "Transfer function of multimode fiber links using an electric field propagation model: Application to Radio over Fibre Systems," Opt. Express **14**(20), 9051–9070 (2006).
18. I. Gasulla and J. Capmany, "Principal mode coefficients for multimode fibers," *in Proceedings of 34th European Conference on Optical Communication ECOC*, (Brussels, Belgium, 2008), pp. 1–2.
19. I. Gasulla and J. Capmany, "Analysis of the harmonic and intermodulation distortion in a multimode fiber optic link," Opt. Express **15**(15), 9366–9371 (2007).

1. Introduction

Microwave photonic (MWP) links featuring low loss, high dynamic range and low noise bring many advantages as compared to traditional microwave links, both in civil and defense fields [1,2]. These advantages have been demonstrated in a variety of applications including signal processing, phased array antennas, radar and radio over fiber systems.

The performance of this kind of links is commonly evaluated in terms of a set of figures of merit (FOM): the radiofrequency (RF) link gain (G_{RF}), the noise figure (*NF*) and the spurious free dynamic range (*SFDR*) [3]. These performance metrics have been computed for a wide variety of configurations [3–9]. In principle, the interest was focused on simple and passive intensity modulated direct detection (IM-DD) point-to-point links (subject to either direct or external modulation) and models were developed providing a detailed description of the effects of the electronic biasing circuits and impedance matching networks [3].

With the development of new photonic technologies and components, more complex MWP links including new optical devices, modulation and detection techniques have started to be considered [4–12]. For instance, IM-DD MWP links including optical amplification have been proposed to provide low RF loss or even gain [4] and, recently, links combining phase modulation and differential delay detection have been considered to enhance the dynamic range [5]. Furthermore, it is envisaged that this trend will not stop here but rather will be expanded to accommodate more advanced features such as, for instance, multiport MWP links whereby a common signal from a central station is sent to different base stations or where different RF signals are sent to different base stations by means of wavelength division multiplexing (WDM). Other examples focus on frequency modulation direct-detection (FM-DD) links [6] as well as on the use of frequency [10] or phase [12] modulation combined with a photonic frequency discriminator to enhance the dynamic range.

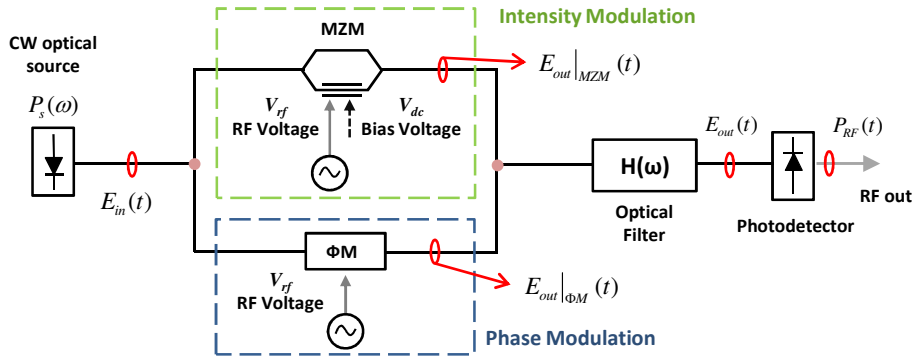

Fig. 1. Schematic of a general single-port filtered MWP link.

#151909 - $15.00 USD Received 27 Jul 2011; revised 28 Aug 2011; accepted 31 Aug 2011; published 23 Sep 2011

All the former examples and also traditional simple MWP links can be represented by the general model shown in Fig. 1 for a single-port system where either intensity or phase modulation (or both simultaneously) can be applied. The effect of all intermediate optical components placed between the electrooptical (EO) and the optical-to-electronic (OE) conversion stages can be lumped into an optical transfer function $H(\omega)$ connecting the input to the output of the system. We use the term *filtered MWP links* to address these systems. Reference [6] similarly considers the inclusion of an arbitrary optical filter, acting as an FM discriminator, for the particular case of directly modulated FM-DD links.

The objective of this paper is to provide the expressions leading to the computation of G_{RF}, *NF* and *SFDR* in general externally modulated filtered MWP links. Special attention must be focused on the fact that many previous FOM analyses consider a monochromatic light source, while many light sources under consideration for optical communications systems are far from being monochromatic [13]. In that context, an exception is found in [8] where the use of non-monochromatic optical sources in IM-DD analog link architectures is accomplished by replacing the standard CW laser by a pulsed optical source. Our model will work under very general conditions for the coherence properties of the optical source, only restricted by the assumption that the source fluctuations can be regarded as a stationary random process.

To our knowledge, these expressions for the main performance criteria are not available in the literature and can be useful since FOM results for complex MWP links can be directly obtained just by substituting the numerical or measured optical transfer function characterizing the link in the overall closed-form expressions.

The paper is organized as follows. In section 2 we provide the closed-form expressions of the figures of merit considering both IM-DD and phase modulation followed by either a single or a balanced detection design. Different examples are developed in section 3 showing the coincidence of the results provided by this model with previously reported expressions of particular links. We also elaborate on the extension of the model to multiport MWP links. Section 4 deals with an example for a MWP link composed of a dispersive either singlemode or multimode fiber link followed by a Fiber Bragg Grating (FBG) notch filter, the spectrum of which is provided by experimental measurement. Finally, our main conclusions and summary are provided in section 5.

2. Analytical model: Derivation of the general figures of merit

The performance metrics for simple unamplified MWP links comprising an optical source, an intensity modulator followed by a photodiode or well a phase modulator with interferometric detection architecture have been derived for both IM-DD [3–5] and phase modulation (ΦM) [5] formats. The inclusion of an optical amplifying stage in analog IM-DD links has been analyzed in [9] for the case when a low-biased Mach-Zehnder modulator (MZM) is followed by an erbium-doped fiber amplifier (EDFA), while optical amplification prior to modulation has been considered in class-B [10] and class-AB [7] MWP links, both of which are focused on enhancing the SFDR providing linear and low-noise transmission. The presence of more complex device configurations in the photonic domain, modeled by means of a lumped optical filter and characterized by an optical transfer function $H(\omega)$, will be developed in this section independently for IM-DD and phase modulation with both single and balanced detection systems.

The linear end-to-end RF gain (or loss) of a representative filtered MWP link, as the one illustrated in Fig. 1, is defined as the ratio of the RF power (at the modulating angular frequency Ω) delivered to a matched load at the photodetector output, $P_{RF}|_{out}$, to the available RF power at the input (at the modulating angular frequency Ω), $P_{RF}|_{in}$, delivered to the modulation device [3]: $G_{RF} = P_{RF}|_{out}(\Omega) / P_{RF}|_{in}(\Omega)$. For both modulation processes we will have $P_{RF}|_{in} = V_{rf}^{\ 2}/(2R_{in})$, where V_{rf} is the amplitude of the voltage signal applied to the external modulator and R_{in} is the input resistance.

#151909 - $15.00 USD Received 27 Jul 2011; revised 28 Aug 2011; accepted 31 Aug 2011; published 23 Sep 2011

The evaluation of the degradation experienced by the microwave signal due to the existing noise sources will be accomplished by evaluating the noise figure parameter as $NF = N_{tot} / (G_{RF}\, N_{in})$, being N_{tot} and N_{in}, respectively, the total output and input noise spectral densities. The NF will be referred to the total relative intensity noise parameter (RIN_{tot}) [4], defined as $RIN_{tot} = N_{tot} / (I|_{dc}^{2}\, R_{out})$, where $I|_{dc}$ represents the DC photocurrent and R_{out} is the output resistance. The RIN_{tot} has been derived taking into account the input and output thermal noises, the shot noise and laser noise contributions: $RIN_{tot} = RIN_{i,th} + RIN_{o,th} + RIN_{shot} + RIN_{laser}$.

For the dynamic range evaluation we will resort to a common figure of merit, the spurious free dynamic range, widely used to simultaneously characterize the linearity and noise characteristics of microwave devices, analogue-to-digital converters and optical devices such as laser diodes and external modulators. The SFDR is defined as the carrier-to-noise ratio when the noise floor in the signal bandwidth equals to the power of a given order intermodulation product. The SFDR of a link limited by second (IMD_2) or third-order (IMD_3) intermodulation distortion can be computed respectively from $SFDR_2 = (OIP_2/N_{tot})^{1/2}$ or $SFDR_3 = (OIP_3/N_{tot})^{2/3}$, where OIP_2 and OIP_3 are the linearly extrapolated input powers at which the fundamental and, respectively, the IMD_2 or IMD_3 output powers would be equal.

2.1. Filtered IM-DD links

We consider a general filtered IM-DD link, as that shown in Fig. 1, assuming that the light source emits a signal whose amplitude, separating the rapid sinusoidal oscillations at the central angular frequency ω_0 from the slower source fluctuations $A(t)$ [13], can be described by $E_{in}(t) = (2P_0)^{1/2}\, e^{j\omega_0 t}\, A(t)$, where P_0 is the optical power at ω_0.

When the modulating signal is composed of a RF tone characterised by an angular frequency Ω, the optical field at the output of one arm of the push-pull MZM is given by

$$E_{out}\big|_{MZM}(t) = j\sqrt{\alpha_{MZM}}\, E_{in}(t)\sin\left[\phi_{dc}/2 + \phi_{rf}/2\sin(\Omega t)\right] \tag{1}$$

where α_{MZM} is the MZM optical loss while $\phi_{rf} = \pi V_{rf}/V_\pi$ and $\phi_{dc} = \pi V_{dc}/V_\pi$ for the bias voltage V_{dc}. After expansion of Eq. (1) in terms of Bessel functions of the first kind, the amplitude spectrum of the modulated signal is obtained as

$$E_{out}\big|_{MZM}(\omega) = 2\pi\sqrt{\alpha_{MZM}}\sum_{n=-\infty}^{\infty} B_n J_n(\phi_{rf}/2)\, E_{in}(\omega - n\Omega) \tag{2}$$

with

$$B_n = (-1)^n\, j^{|n|+1}\sin(\phi_{dc}/2 + |n|\,\pi/2), \tag{3}$$

where at the modulator quadrature bias point one must set $\phi_{dc} = \pi/2$.

We will need the autocorrelation function of the spectrum, given from Eq. (2) as

$$\left\langle E_{out}\big|_{MZM}(\omega)\, E_{out}^{*}\big|_{MZM}(\omega')\right\rangle = (2\pi)^2\,\alpha_{MZM}\, 2P_0\sum_{n=-\infty}^{\infty}\sum_{m=-\infty}^{\infty} B_n B_m^{*} J_n(\phi_{rf}/2)\, J_m(\phi_{rf}/2)\, P_s(\omega - \omega_0 + n\Omega)\,\delta\left[\omega' - (\omega + (n-m)\Omega)\right] \tag{4}$$

where the symbol < > indicates an ensemble average. $P_s(\omega)$ is the spectral density function of the optical source, usually modeled as a Gaussian [13,14,16], or Lorentzian function, which is defined as the Fourier transform of the temporal autocorrelation function $R(u)$:

$$P_s(\omega) = \int_{-\infty}^{\infty} R(u)\, e^{-i\omega u}\, du \tag{5}$$

#151909 - $15.00 USD Received 27 Jul 2011; revised 28 Aug 2011; accepted 31 Aug 2011; published 23 Sep 2011

being the source fluctuations regarded as a stationary random process so that their temporal autocorrelation function can be written as $< A(t)\, A^*(t') > = R(t-t')$.

The ensemble average power of light after propagation through a general optical filter, characterized by its optical transfer function $H(\omega)$, can be expressed in terms of the autocorrelation function of the spectrum at the filter output as follows

$$\left\langle P(t)\right\rangle = \frac{1}{(2\pi)^2}\int_{-\infty}^{\infty}\int_{-\infty}^{\infty}\left\langle E_{out}(\omega)E_{out}^{*}(\omega')\right\rangle e^{j(\omega-\omega')t}d\omega d\omega' =$$

$$\alpha_{MZM}\,2P_0\sum_{n=-\infty}^{\infty}\sum_{m=-\infty}^{\infty}B_nB_m^{*}J_n(\phi_{rf}/2)J_m(\phi_{rf}/2)e^{-j(n-m)\Omega t}\int_{-\infty}^{\infty}P_s(\omega-\omega_0+n\Omega)H(\omega)H^{*}\left[\omega+(n-m)\Omega\right]d\omega \tag{6}$$

Assuming small-signal approximation, the RF photodetected power for the signal contribution is developed as

$$P_{RF}^{I}\Big|_{out}(\Omega) = 2I_{dc}{}^2R_{out}\left(\phi_{rf}/4\right)^2\sin^2(\phi_{dc})\left|A_{\Omega}^{I}\right|^2 \tag{7}$$

where I_{dc} is defined as $I_{dc} = \Re\,\alpha_{MZM}\,P_0/2$ for a photodetector responsivity $\Re$, as in [5], and

$$A_{\Omega}^{I} = \sum_{n=\{0,1\}}\int_{-\infty}^{\infty}P_s(\omega-\omega_0-n\Omega)H(\omega)H^{*}(\omega-\Omega)d\omega. \tag{8}$$

In consequence, Eq. (7) implies an end-to-end RF link gain given by

$$G_{RF}^{I}(\Omega) = \left(I_{dc}\pi/V_{\pi}\right)^2\sin^2(\phi_{dc})R_{in}R_{out}\left|A_{\Omega}^{I}/2\right|^2. \tag{9}$$

In relation to the link noise characterization and taking into account the definition of RIN_{tot}, we obtain the following expressions for the *NF*, as well as for the *RIN* terms referenced to the output due to thermal noise at the input, thermal noise at the output, and shot noise

$$NF^{I} = 4\frac{RIN_{tot}V_{\pi}{}^2}{\pi^2R_{in}k_BT}\frac{\left[1-\cos(\phi_{dc})\right]^2}{\sin^2(\phi_{dc})}\frac{\left|A_{DC}^{I}\right|^2}{\left|A_{\Omega}^{I}\right|^2}, \tag{10}$$

$$RIN_{i,th}^{I} = \frac{k_BT\pi^2R_{in}}{4V_{\pi}{}^2}\frac{\sin^2(\phi_{dc})}{\left[1-\cos(\phi_{dc})\right]^2}\frac{\left|A_{\Omega}^{I}\right|^2}{\left|A_{DC}^{I}\right|^2}, \tag{11}$$

$$RIN_{o,th}^{I} = \frac{k_BT}{I_{dc}{}^2R_{out}}\frac{1}{\left[1-\cos(\phi_{dc})\right]^2\left|A_{DC}^{I}\right|^2} \quad \text{and} \tag{12}$$

$$RIN_{shot}^{I} = \frac{2e}{I_{dc}}\cdot\frac{1}{\left[1-\cos(\phi_{dc})\right]\left|A_{DC}^{I}\right|}. \tag{13}$$

being k_B the Boltzmann constant, T the temperature, e the electronic charge constant and

$$A_{DC}^{I} = \int_{-\infty}^{\infty}P_s(\omega-\omega_0)\left|H(\omega)\right|^2d\omega. \tag{14}$$

For the dynamic range evaluation we assume a modulating signal composed of two RF tones, characterised by the same amplitude V_{rf} at angular frequencies Ω_1 and Ω_2. In principle, one is primarily concerned with the $SFDR_3$ related to the products placed at $2\Omega_1 - \Omega_2$ or $2\Omega_2 - \Omega_1$, as in any MWP link these frequencies may appear within the system bandwidth. On the

#151909 - $15.00 USD Received 27 Jul 2011; revised 28 Aug 2011; accepted 31 Aug 2011; published 23 Sep 2011

other hand, the $SFDR_2$ becomes also important for systems whose bandwidth is more than one octave since the IMD_2 products at $\Omega_1 \pm \Omega_2$ will then fall outside the passband of a suboctave link. We will discuss both broadband and suboctave MWP links.

The expression for the photodetected RF power relative to the IMD_2 term placed at the angular frequency $\Omega_1 \pm \Omega_2$ is obtained as

$$P_{RF}^{I}\Big|_{out}(\Omega_1 \pm \Omega_2) = 2{I_{dc}}^2 R_{out}\left(\phi_{rf}/4\right)^4 \left|A^{I}_{\Omega_1 \pm \Omega_2}\right|^2 \tag{15}$$

where, similarly to Eq. (8), we define

$$A^{I}_{\Omega_1 \pm \Omega_2} = \pm \sum_{\substack{n=\{0,1\}\\ m=\{-1,0\}}} \left[(-1)^{n+m} - \cos(\phi_{dc})\right] \int_{-\infty}^{\infty} P_s(\omega - \omega_0 - n\Omega_1 \pm m\Omega_2) H(\omega) H^*(\omega - \Omega_1 \mp \Omega_2) d\omega. \tag{16}$$

Given Eq. (7) and (15), which lead the calculation of the OIP_2 value, we can express the $SFDR_2$ in terms of the RIN_{tot} parameter as:

$$SFDR_2^I = \sqrt{\frac{2}{RIN_{tot}}} \frac{\sin^2(\phi_{dc})}{\left|1-\cos(\phi_{dc})\right|} \frac{\left|A^{I}_{\Omega_1}\right|^2}{\left|A^{I}_{\Omega_1 \pm \Omega_2}\right|\left|A^{I}_{DC}\right|}. \tag{17}$$

And in a similar way for the 3rd-order intermodulation distortion term at $2\Omega_1 - \Omega_2$, we have

$$P_{RF}^{I}\Big|_{out}(2\Omega_1 - \Omega_2) = 2{I_{dc}}^2 R_{out}\left(\phi_{rf}/4\right)^6 \sin^2(\phi_{dc}) \left|A^{I}_{2\Omega_1 - \Omega_2}\right|^2 \tag{18}$$

with

$$A^{I}_{2\Omega_1 - \Omega_2} = \sum_{\substack{n=\{0,1,2\}\\ m=\{-1,0\}}} \left(1/2\right)^{|n-1|} \int_{-\infty}^{\infty} P_s(\omega - \omega_0 - n\Omega_1 - m\Omega_2) H(\omega) H^*(\omega - 2\Omega_1 + \Omega_2) d\omega \tag{19}$$

which results in

$$SFDR_3^I = \left[\frac{2}{RIN_{tot}} \frac{\sin^2(\phi_{dc})}{\left|1-\cos(\phi_{dc})\right|} \frac{\left|A^{I}_{\Omega_1}\right|^3}{\left|A^{I}_{2\Omega_1 - \Omega_2}\right|\left|A^{I}_{DC}\right|^2}\right]^{2/3}. \tag{20}$$

Note that if the optical source can be assumed as monochromatic and, subsequently, the spectral density function of the source $P_s(\omega)$ approximated by a delta function, Eq. (8), (14), (16) and (19) result in

$$A^{I}_{\Omega}\Big|_{\delta} = \sum_{n=\{0,1\}} H(\omega_0 + n\Omega) H^*\left[\omega_0 + (n-1)\Omega\right], \tag{21}$$

$$A^{I}_{DC}\Big|_{\delta} = \left|H(\omega_0)\right|^2, \tag{22}$$

$$A^{I}_{\Omega_1 \pm \Omega_2}\Big|_{\delta} = \pm \sum_{\substack{n=\{0,1\}\\ m=\{-1,0\}}} \left[(-1)^{n+m} - \cos(\phi_{dc})\right] H(\omega_0 + n\Omega_1 \mp m\Omega_2) H^*\left[\omega_0 + (n-1)\Omega_1 \mp (m+1)\Omega_2\right] \tag{23}$$

and

$$A^{I}_{2\Omega_1 - \Omega_2}\Big|_{\delta} = \sum_{\substack{n=\{0,1,2\}\\ m=\{-1,0\}}} \left(1/2\right)^{|n-1|} H(\omega_0 + n\Omega_1 + m\Omega_2) H^*\left[\omega_0 + (n-2)\Omega_1 + (m+1)\Omega_2\right]. \tag{24}$$

#151909 - $15.00 USD Received 27 Jul 2011; revised 28 Aug 2011; accepted 31 Aug 2011; published 23 Sep 2011

It must be noted that if we consider a back-to-back configuration where we can omit the presence of the optical filter by setting $H(\omega) = 1$ for every frequency, our IM-DD model provides exactly the same expressions for G_{RF}, the different *RIN* contributions, *NF* and *SFDR* for 3rd-order intermodulation that those previously reported in [5] by Urick et al. for external intensity modulation of a monochromatic optical source.

2.2. Filtered Phase modulated links with both balanced and single detection

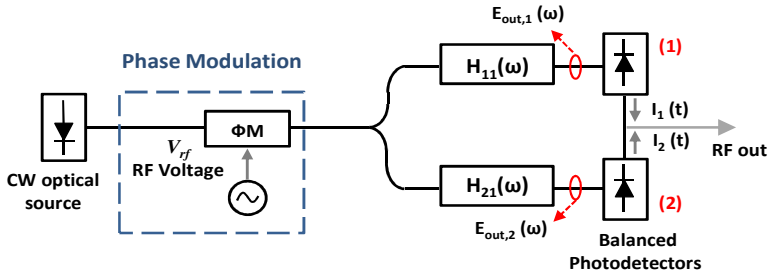

Fig. 2. Schematic of a filtered MWP link applying phase modulation with a general balanced detection scheme.

The procedure followed for the performance analysis of filtered phase modulated links is similar as that previously employed for filtered IM-DD links, where now the output of the phase modulator is

$$E_{out}\big|_{\Phi M}(t) = j\sqrt{\alpha_{\Phi M}}\,E_{in}(t)e^{j\phi_{rf}\sin(\Omega t)} \tag{25}$$

being $\alpha_{\Phi M}$ the phase modulator insertion loss.

As represented in Fig. 2, we will consider a general case for balanced photodetection where each detector is preceded by a different optical filter, $H_{11}(\omega)$ and $H_{21}(\omega)$, and calculate the photodetected total current subtracting the current obtained in the second detector from the one corresponding to the first: $I(t) = I_1(t) - I_2(t)$.

The RF photodetected power and link gain are then respectively derived as

$$P_{RF}^{\Phi}\big|_{out}(\Omega) = 2{I_{dc}}^2 R_{out}{\phi_{rf}}^2\left|A_{\Omega}^{\Phi}\right|^2 \tag{26}$$

where

$$A_{\Omega}^{\Phi} = \sum_{n=\{0,1\}}(-1)^n\int_{-\infty}^{\infty}P_s(\omega-\omega_0-n\Omega)\left[H_{11}(\omega)H_{11}^*(\omega-\Omega)-H_{21}(\omega)H_{21}^*(\omega-\Omega)\right]d\omega \tag{27}$$

and

$$G_{RF}^{\Phi}(\Omega) = 4\left(I_{dc}\pi/V_{\pi}\right)^2 R_{in}R_{out}\left|A_{\Omega}^{\Phi}\right|^2. \tag{28}$$

For modelling of the involved noise metrics in the balanced detection scheme under evaluation, we will take into account that the noise current contributions add incoherently in the balanced detection process, and subsequently refer them to the total relative intensity noise as $RIN_{tot} = N_{tot} / (I|_{dc}^2\, R_{out})$, where $I|_{dc}$ is defined for convenience as the sum of the DC photocurrents provided by both detectors: $I|_{dc} = I_1|_{dc} + I_2|_{dc} = 2\,I_{dc}\,A_{DC}^{\Phi}$, for

$$A_{DC}^{\Phi} = \int_{-\infty}^{\infty}P_s(\omega-\omega_0)\left[\left|H_{11}(\omega)\right|^2+\left|H_{21}(\omega)\right|^2\right]d\omega \tag{29}$$

consequently obtaining

#151909 - $15.00 USD Received 27 Jul 2011; revised 28 Aug 2011; accepted 31 Aug 2011; published 23 Sep 2011

$$NF^{\Phi} = \frac{RIN_{tot} V_{\pi}^{\,2}}{\pi^2 R_{in} k_B T} \frac{\left|A_{DC}^{\Phi}\right|^2}{\left|A_{\Omega}^{\Phi}\right|^2}, \tag{30}$$

$$RIN_{o,th}^{\Phi} = \frac{k_B T}{4 I_{dc}^{\,2} R_{out}} \cdot \frac{1}{\left|A_{DC}^{\Phi}\right|^2}, \tag{31}$$

$$RIN_{i,th}^{\Phi} = \frac{k_B T \pi^2 R_{in}}{V_{\pi}^{\,2}} \cdot \frac{\left|A_{\Omega}^{\Phi}\right|^2}{\left|A_{DC}^{\Phi}\right|^2} \quad \text{and} \tag{32}$$

$$RIN_{shot}^{\Phi} = \frac{e}{I_{dc}} \cdot \frac{1}{\left|A_{DC}^{\Phi}\right|}. \tag{33}$$

The IMD_2 output power and $SFDR_2$ correspond, respectively, to

$$P_{RF}^{\Phi}\Big|_{out}(\Omega_1 \pm \Omega_2) = \frac{I_{dc}^{\,2} R_{out}}{2} \phi_{rf}^{\,4} \left|A_{\Omega_1 \pm \Omega_2}^{\Phi}\right|^2 \tag{34}$$

with

$$A_{\Omega_1 \pm \Omega_2}^{\Phi} = \pm \sum_{\substack{n=\{0,1\} \\ m=\{-1,0\}}} (-1)^{n+m} \int_{-\infty}^{\infty} P_s(\omega - \omega_0 - n\Omega_1 \pm m\Omega_2) \left[H_{11}(\omega) H_{11}^{*}(\omega - \Omega_1 \mp \Omega_2) - H_{21}(\omega) H_{21}^{*}(\omega - \Omega_1 \mp \Omega_2) \right] d\omega \tag{35}$$

and

$$SFDR_2^{\Phi} = \sqrt{\frac{2}{RIN_{tot}}} \frac{\left|A_{\Omega_1}^{\Phi}\right|^2}{\left|A_{\Omega_1 \pm \Omega_2}^{\Phi}\right| \left|A_{DC}^{\Phi}\right|}. \tag{36}$$

Finally, for 3rd-order intermodulation distortion we obtain

$$P_{RF}^{\Phi}\Big|_{out}(2\Omega_1 - \Omega_2) = \frac{I_{dc}^{\,2} R_{out}}{8} \phi_{rf}^{\,6} \left|A_{2\Omega_1 - \Omega_2}^{\Phi}\right|^2 \tag{37}$$

where

$$A_{2\Omega_1 - \Omega_2}^{\Phi} = \sum_{\substack{n=\{0,1,2\} \\ m=\{-1,0\}}} (1/2)^{|n-1|} (-1)^m \int_{-\infty}^{\infty} P_s(\omega - \omega_0 - n\Omega_1 - m\Omega_2) \left[H_{11}(\omega) H_{11}^{*}(\omega - 2\Omega_1 + \Omega_2) - H_{21}(\omega) H_{21}^{*}(\omega - 2\Omega_1 + \Omega_2) \right] d\omega \tag{38}$$

and finally

$$SFDR_3^{\Phi} = \left[\frac{4}{RIN_{tot}} \frac{\left|A_{\Omega_1}^{\Phi}\right|^3}{\left|A_{2\Omega_1 - \Omega_2}^{\Phi}\right| \left|A_{DC}^{\Phi}\right|^2} \right]^{2/3}. \tag{39}$$

The above developed model can be directly applied to phase modulated single-port links where only a single photodetector is used in the detection stage by merely forcing $H_{21}(\omega) = 0$.

Note again that if the spectral density function of the source $P_s(\omega)$ can be approximated by a delta function, Eq. (27), (29), (35) and (38) result in

#151909 - $15.00 USD Received 27 Jul 2011; revised 28 Aug 2011; accepted 31 Aug 2011; published 23 Sep 2011

$$A_{\Omega}^{\Phi}\Big|_{\delta} = \sum_{n=\{0,1\}} (-1)^n \left[H_{11}(\omega_0 + n\Omega) H_{11}^*(\omega_0 + (n-1)\Omega) - H_{21}(\omega_0 + n\Omega) H_{21}^*(\omega_0 + (n-1)\Omega) \right], \tag{40}$$

$$A_{DC}^{\Phi}\Big|_{\delta} = \left| H_{11}(\omega_0) \right|^2 + \left| H_{21}(\omega_0) \right|^2, \tag{41}$$

$$A_{\Omega_1 \pm \Omega_2}^{\Phi}\Big|_{\delta} = \pm \sum_{\substack{n=\{0,1\} \\ m=\{-1,0\}}} (-1)^{n+m} \left[H_{11}(\omega_0 + n\Omega_1 \mp m\Omega_2) H_{11}^*(\omega_0 + (n-1)\Omega_1 \mp (m+1)\Omega_2) \right.$$
$$\left. - H_{21}(\omega_0 + n\Omega_1 \mp m\Omega_2) H_{21}^*(\omega_0 + (n-1)\Omega_1 \mp (m+1)\Omega_2) \right] \tag{42}$$

and

$$A_{2\Omega_1 - \Omega_2}^{\Phi}\Big|_{\delta} = \sum_{\substack{n=\{0,1,2\} \\ m=\{-1,0\}}} (1/2)^{|n-1|} (-1)^m \left\{ H_{11}(\omega_0 + n\Omega_1 + m\Omega_2) \left[H_{11}^* \omega_0 + (n-2)\Omega_1 + (m+1)\Omega_2 \right] \right.$$
$$\left. - H_{21}(\omega_0 + n\Omega_1 + m\Omega_2) - H_{21}^* \left[\omega_0 + (n-2)\Omega_1 + (m+1)\Omega_2 \right] \right\}. \tag{43}$$

3. Analytical model: discussion and particularization

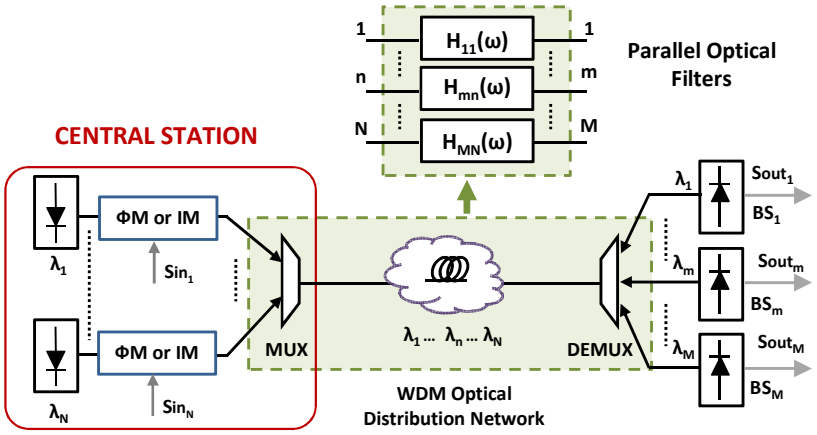

Fig. 3. Multiport filtered MWP link implementing WDM distribution.

The principal advantage of our model relies on the global character of the developed figures of merit, which allows the potential application to an extensive variety of MWP transmission systems. In this sense, an important area of interest constitute multiport radio over fiber systems where, either an electrical common signal or a multiplex of independent channels, are distributed to a set of different base stations (BS_m). Figure 3 depicts an schematic of WDM transmission in a multiport MWP link whose optical distribution network can be substituted for a bank of parallel optical filters, where $H_{mn}(\omega)$ represents the optical transfer function between output port m (output signal $Sout_m$) and input port n (output signal Sin_n).

As a proof of concept, different examples representing typical MWP layouts are now considered, where our model will be successfully applied just by substituting the known expressions for the equivalent optical transfer function $H(\omega)$ in the final FOM developed formulas. In particular, we will focus on a particularization of multiport MWP links to interferometric balanced photodetection and also on a dispersive fiber link, considering both standard singlemode (SMF) and multimode (MMF) fiber transmission.

#151909 - $15.00 USD Received 27 Jul 2011; revised 28 Aug 2011; accepted 31 Aug 2011; published 23 Sep 2011

3.1. Phase modulation with interferometric detection

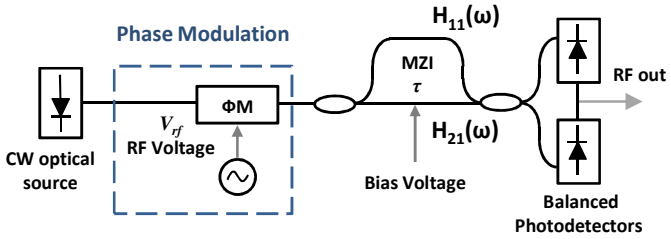

Fig. 4. Phase modulation with interferometric detection scheme.

The particularization of the model to the case of phase modulation with the interferometric balanced detection architecture shown in Fig. 4, can be performed if the inclusion of the asymmetric Mach-Zehnder interferometer (MZI) prior to the balanced detection process is properly characterized by the following expressions for both parallel optical filters:

$$H_{11}(\omega)\big|_{MZI} = j\sqrt{\alpha_{MZI}}\,e^{j\omega\tau/2}\sin(\omega\tau/2) \quad \text{and} \quad H_{21}(\omega)\big|_{MZI} = j\sqrt{\alpha_{MZI}}\,e^{j\omega\tau/2}\cos(\omega\tau/2), \quad (44)$$

where α_{MZI} is the MZI insertion loss and τ is the differential time delay in the MZI. The FOM expressions derived from our model for a monochromatic optical source show an exact coincidence with those reported in [5] where the MZI was set at quadrature by applying $\omega_0\tau = \pi/2$. In this case the formulas for G_{RF}, NF and the different RIN parameters correspond to

$$G_{RF}^{\Phi}(\Omega)\big|_{MZI} = 16\left(I_{dc}\alpha_{MZI}\pi/V_{\pi}\right)^2 R_{in}R_{out}\sin^2(\Omega\tau/2), \quad (45)$$

$$NF^{\Phi}\big|_{MZI} = \frac{RIN_{tot}V_{\pi}^{\,2}}{4\pi^2 R_{in}k_B T\sin^2(\Omega\tau/2)}, \quad (46)$$

$$RIN_{o,th}^{\Phi}\big|_{MZI} = \frac{k_B T}{4I_{dc}^{\,2}\alpha_{MZI}^{\,2}R_{out}}, \quad RIN_{i,th}^{\Phi}\big|_{MZI} = \frac{4k_B T\pi^2 R_{in}}{V_{\pi}^{\,2}} \quad \text{and} \quad RIN_{shot}^{\Phi}\big|_{MZI} = \frac{e}{I_{dc}\alpha_{MZI}}. \quad (47)$$

Since we are working under MZI quadrature conditions, the 2nd-order intermodulation distortion is null while for the 3rd-order one we obtain

$$SFDR_3^{\Phi}\big|_{MZI} = \left[\frac{4}{RIN_{tot}}\cdot\frac{1-\cos(\Omega_1\tau)}{\left|\cos\left[(\Omega_1-\Omega_2)\tau/2\right]-\cos\left[(\Omega_1+\Omega_2)\tau/2\right]\right|}\right]^{2/3}. \quad (48)$$

that can be approximated to $SFDR_3^{\Phi}\big|_{MZI} = \left(4/RIN_{tot}\right)^{2/3}$ if working near the peak of the G_{RF} response where Ω_1 tends to Ω_2, as described in [5].

3.2. Singlemode and Multimode Dispersive Microwave Photonic links

A common example of practical interest is found in 2nd-order dispersive links where the propagation constant $\beta(\omega)$ can be expanded in a Taylor's series around the central angular frequency ω_0 as

$$\beta(\omega) \approx \beta(\omega_0) + \left.\frac{d\beta(\omega)}{d\omega}\right|_{\omega=\omega_0}(\omega-\omega_0) + \frac{1}{2}\left.\frac{d\beta^2(\omega)}{d\omega^2}\right|_{\omega=\omega_0}(\omega-\omega_0)^2 = \beta^0 + \beta'(\omega-\omega_0) + \frac{1}{2}\beta''(\omega-\omega_0)^2. \quad (49)$$

Moreover, we consider an optical source represented by a Gaussian power spectrum $P_s(\omega)$ with a root mean square (RMS) linewidth ΔW related to the source RMS coherence time as $\Delta W = 1/(\sqrt{2}\sigma_c)$:

#151909 - $15.00 USD Received 27 Jul 2011; revised 28 Aug 2011; accepted 31 Aug 2011; published 23 Sep 2011

$$P_s(\omega) = P_0 \frac{\sqrt{\pi}}{\Delta W} e^{\frac{-\omega^2}{(2\Delta W)^2}}. \quad (50)$$

For a SMF link of length L, for which we assume that the power optical loss $\alpha(\omega)$ is independent of ω, i.e. $\alpha(\omega) \approx \alpha(\omega_0) = \alpha^0$, we must apply the optical transfer function

$$H\big|_{SMF}(\omega) = e^{-\alpha^0 L/2} e^{-j\left[\beta^0 + \beta'(\omega-\omega_0) + \beta''/2(\omega-\omega_0)^2\right]L}, \quad (51)$$

in the described theory to directly obtain the characterization of the figures of merit of interest. For instance, the substitution of Eq. (50) and (51) in the closed-form expressions for the RF gain both in intensity, Eq. (9), and phase, Eq. (28), modulated MWP links with single-detection architecture, give us the following well-known closed-form equations

$$G^I_{RF}(\Omega)\big|_{SMF} = \left(I_{dc}\pi / V_\pi\right)^2 \sin^2(\phi_{dc}) R_{in} R_{out} e^{-2\left(\beta'' L \Omega \Delta W\right)^2} \cos^2\left(\beta'' \Omega^2 L/2\right) e^{-2\alpha^0 L} \quad \text{and} \quad (52)$$

$$G^\Phi_{RF}(\Omega)\big|_{SMF} = \left(4 I_{dc}\pi / V_\pi\right)^2 R_{in} R_{out} e^{-2\left(\beta'' L \Omega \Delta W\right)^2} \sin^2\left(\beta'' \Omega^2 L/2\right) e^{-2\alpha^0 L}. \quad (53)$$

These results are in concordance with previous work related to the characterization of fiber dispersion in intensity [15] and phase modulated [11] MWP systems. As it can be observed in both expressions, the first exponential factor is a low-pass frequency response term which depends on β'' and the spectral source linewidth ΔW. The intermediate factor is the well-known carrier suppression effect (CSE) that is due to the phase offset between the upper and lower modulation sidebands.

In the case of MWP links based on multimode fiber transmission, it is not only required to determine the effect of chromatic dispersion and the temporal source coherence over the microwave signal, but also the magnitude of other relevant sources of impairment as: the intermodal dispersion, the differential modal attenuation, the coupling between the propagated modes and both the coupling from the input signal to the modes at fiber input and from the output signal to the detector area. Traditionally this work has been carried out using the coupled mode theory which requires a complex and lengthy derivation, either by numerical resolution of the coupled power-flow equations [16], or by means of an analytical model based on electric field propagation [17]. However, it has been shown that MMF support the transmission of principal modes (PMs) which do not suffer from modal dispersion to first order of frequency variation and form orthogonal bases both at the input and the output of the fiber. They constitute therefore a useful tool for deriving a more amenable formalism for the analysis of propagation through MMFs [18], as PM theory enable us to express the optical field transfer function of the MMF link in function of its output principal modes $\{|b_m(L)\rangle\}$:

$$H\big|_{MMF}(\omega) = e^{-j\frac{\beta_0''}{2}(\omega-\omega_0)^2 L} \sum_{m=1}^{M} c_m(L)\, \varepsilon_m^b\, |b_m(L)\rangle e^{-\alpha_m^0 L/2} e^{-j\beta_m^0 L} e^{-j\tau_m(\omega-\omega_0)}, \quad (54)$$

where $c_m(L)$ is the (distance-dependent) expansion coefficient corresponding to the m-th PM of amplitude ε_m^b. In this case, α_m^0 is the modal attenuation, β_m^0 the propagation constant and τ_m the modal group delay all dependent on the m-th PM and properly defined in [17], while the 2^{nd} derivative of the propagation constant was considered the same for all the PMs, $\beta_m'' \approx \beta_0''$.

To obtain, in a similar way to the SMF, the expressions leading to the RF link gain it is necessary to calculate the parameters A_Ω^I and A_Ω^Φ, which offer themselves an interpretation of the RF end-to-end transfer function of the link in conjunction with the coherence properties of

#151909 - $15.00 USD Received 27 Jul 2011; revised 28 Aug 2011; accepted 31 Aug 2011; published 23 Sep 2011

the light source for both intensity and phase modulation approaches. They can be respectively deduced from Eq. (8) and (27) as

$$A_{\Omega}^{I}\Big|_{MMF} = 2e^{-\left(\beta_0' L\Omega\Delta W\right)^2}\cos\left(\beta_0'' \Omega^2 L/2\right)\sum_{m=1}^{M} 2m\left(C_{mm}+G_{mm}\right)e^{-\alpha_m^0 L}e^{-j\tau_m\Omega} \quad \text{and} \quad (55)$$

$$A_{\Omega}^{\Phi}\Big|_{MMF} = 2je^{-\left(\beta_0' L\Omega\Delta W\right)^2}\sin\left(\beta_0'' \Omega^2 L/2\right)\sum_{m=1}^{M} 2m\left(C_{mm}+G_{mm}\right)e^{-\alpha_m^0 L}e^{-j\tau_m\Omega}, \quad (56)$$

for which we took into account that $\left\langle b_m(L)\middle| b_{m'}^{*}(L)\right\rangle = \delta_{mm'}$ and conveniently deduced the expansion coefficients as in [18]:

$$\left|c_m\right|^2\left|\varepsilon_m^b\right|^2 = 2m(C_{mm}+G_{mm}), \quad (57)$$

where C_{mm} is the light injection coefficient (see Eq. (5) of [17]) and G_{mm} is the modal-coupling coefficient defined for power transitions only between adjacent mode groups (see Eq. (77) of [17]). We can observe, as expected, that the right-hand side of Eq. (55) and (56) contains the above mentioned low-pass frequency factor dependent on the temporal coherence behavior of the source and also the carrier suppression effect. The third term represents a microwave photonic transversal filtering effect where each sample corresponds to a different PM (or equivalent mode group) m. For IM-DD, $A_{\Omega}^{I}\Big|_{MMF}$ coincides with the expression for the linear RF transfer function of a MMF link developed in [17] using the coupled mode analysis, (see Eq. (73) of [17]). Furthermore, the analysis of the 2^{nd}-order intermodulation distortion provides the same expression for $A_{\Omega_1\pm\Omega_2}^{I}\Big|_{MMF}$ that the one reported in [19] for the ensemble average power of light in the frequency domain when we consider the linear contribution of the optical signal in terms of the linear superposition of the propagated mode groups (instead of including the optical interference caused between the overlapping mode groups).

Other representative systems covered by our definition of *filtered MWP links* can be found in optical links where an optical filter is included prior to detection acting as an FM discriminator that converts FM to IM [6,10,12]. Different approaches has been studied to accomplished this task, including Mach-Zehnder interferometers, FBGs [10], ring-resonators-assisted linearized interferometers [12], as well as complimentary filters in conjunction with balance detection in order to suppress 2^{nd}-order distortion [6,12]. Specifically, the application of our model to an optical intensity linear filter, experiencing a time delay τ, will be performed by simply considering a transfer function $H(\omega) = (A\cdot\omega)^{1/2}\, e^{-j\tau\omega}$, for a slope A, while a filter frequency linear in electrical field would be characterized by setting $H(\omega) = A\cdot\omega\, e^{-j\tau\omega}$. On the other hand, FOM evaluation of filters experiencing complementary slope responses can be reached by properly representing both parallel optical filters in Fig. 2 as

$$H_{11}(\omega_0+\Omega)\Big|_{lin} = A(\omega_0+\Omega)e^{-j(\omega_0+\Omega)\tau} \quad \text{and} \quad H_{21}(\omega_0+\Omega)\Big|_{lin} = A(\omega_0-\Omega)e^{-j(\omega_0+\Omega)\tau}. \quad (58)$$

#151909 - $15.00 USD Received 27 Jul 2011; revised 28 Aug 2011; accepted 31 Aug 2011; published 23 Sep 2011

4. Application case study

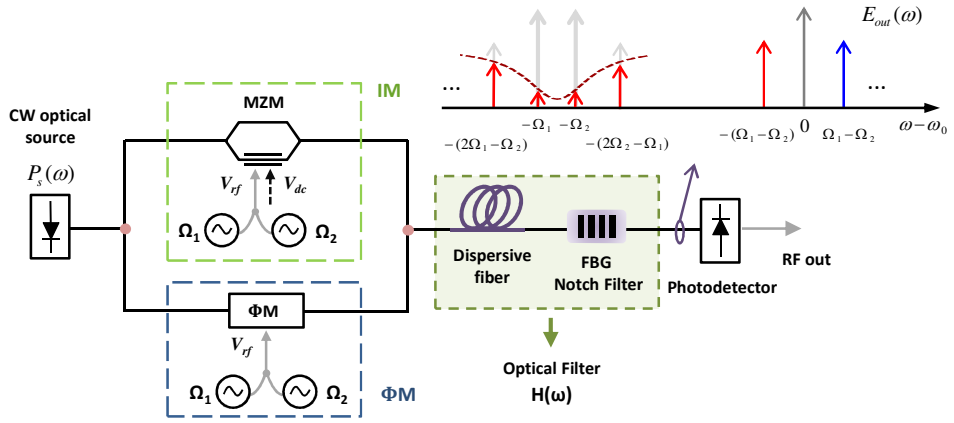

Fig. 5. Schematic of a filtered MWP link composed of a dispersive fiber link and a FBG-based notch filter.

As a proof of concept, the reported analytical model will be applied to the performance evaluation of an interesting application case, represented in Fig. 5, composed of a dispersive fiber link followed by a notch filter implemented by a FBG, the spectrum of which is provided by experimental measurement. The functionality of the selective optical filter is to suppress the lower-frequency sideband of the microwave signal as it has been depicted in the upper region of Fig. 5. We will consider both standard silica SMF and 62.5/125-μm parabolic-core graded-index MMF links characterized by an intrinsic loss α^0 = 0.2 dB/km and $\beta^{''}$ = −21 psec^2/km for an optical wavelength of 1.55 μm. The modal attenuation α_m^0, the modal delay time τ_m the light injection coefficient C_{mm} and the modal coupling coefficient G_{mm} have been calculated following the formulas previously presented in Ref [17]. The equivalent optical transfer function $H(\omega)$ will result in a cascade of the FBG frequency response and the transfer function given by Eq. (51) and Eq. (54) respectively for the SMF and MMF links.

Both intensity and phase modulation with direct-detection will be considered for a modulating signal comprising two RF tones for which we have selected two different combinations of the microwave frequencies f_1 and f_2, involving two different suppression levels for the red-shifted frequency sideband of the electrical signal: an attenuation of around 38.5 dB for both tones if their frequencies are placed at the center of the notch response (namely case FBG$_A$), f_1^A = 12 and f_2^A = 10 GHz; while values around 8 and 11 dB when they are placed in the area corresponding to the frequency slopes of the filter response (referred as case FBG$_B$), f_1^B = 16 and f_2^B = 7 GHz. The measured magnitude and phase shift frequency responses of the FBG operating in transmission are shown in Fig. 6 in function of the difference between the microwave frequency f and the filter central frequency f_c. The relative location of the RF tones in the FBG response has been included in Fig. 6 for both filtering conditions FBG$_A$ and FBG$_B$.

#151909 - $15.00 USD Received 27 Jul 2011; revised 28 Aug 2011; accepted 31 Aug 2011; published 23 Sep 2011

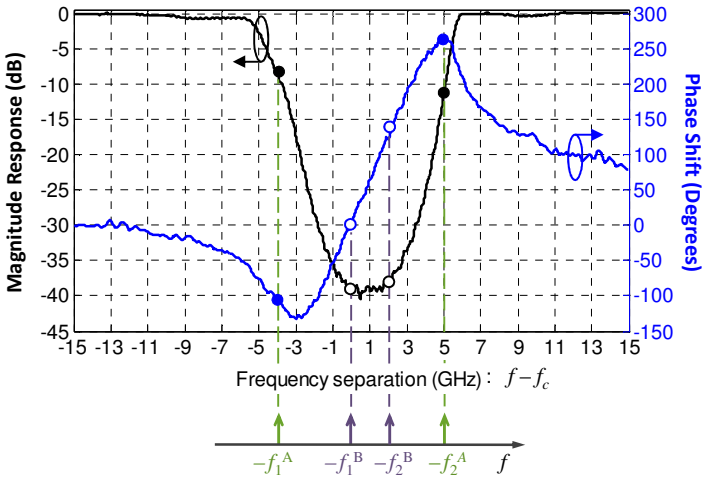

Fig. 6. Measured FBG transmission magnitude and phase shift frequency responses.

The performance analysis of the proposed filtered MWP link is accomplished firstly by evaluating the RF Link Gain frequency response for the particular case where only the dispersive optical fiber is present. With the objective of showing the coincidence of the computed results with previously reported expressions for this well-known radio over fiber system, we report a comparison between singlemode propagation, represented in Fig. 7 (a) and (b), and multimode transmission, gathered in Fig. 7 (c) - (f), for different application contexts. The dependence of the link gain on the coherence properties of a Gaussian optical source is corroborated by comparing two representative RMS spectral linewidths, Δf = 10 MHz and 4 GHz, where $\Delta W = 2\pi \cdot \Delta f$. The influence of both the CSE and the multimode transversal filtering effect is evaluated by considering different link lengths, L = 5 km, [Fig. 7 (a), (c), (e)], and L = 20 km, [Fig. 7 (b), (d), (f)]. The following parameters are kept fixed: V_π = 6.9 V, quadrature MZM bias point $\phi_{dc} = \pi/2$, I_{dc} = 5 mA and $R_{in} = R_{out}$ = 50 Ω.

We initiate the G_{RF} evaluation for this well-known dispersive fiber link by analyzing the main differences in between the frequency responses offered by the two modulation formats under consideration. As it was expected, we can see at first glance for every example gathered in Fig. 7, the influence of the CSE and how the gain notches are produced at different frequency locations when comparing both modulation techniques. This characteristic can be derived for SMF from Eq. (52) and (53) and also for MMF according to Eq. (55) and (56). These equations predict also the 12-dB difference between the peak levels, mainly appreciable for L = 20 km, in total agreement with [5]. It should be also mentioned that, as predicted, in principle transmission regions can be identified in both single and multimode propagation for L = 5 km while for L = 20 km the effect of the carrier suppression term cannot be overlooked.

The reported expression for G_{RF} in terms of the spectral density function of the optical source can be employed to efficiently investigate the effect of its coherence properties on our system performance. As we can observe, the source dependent low-pass frequency term present in Eq. (52) and (53) for the SMF and in Eq. (55) and (56) for the MMF becomes patent when we increase the source spectral linewidth from Δf = 10 MHz, typical of a distributed feedback laser (DFB), up to a value of Δf = 9 GHz, for a 20 km link length. The same low-pass behavior, previously discussed in [17], occurs for both single and multimode fibers.

#151909 - $15.00 USD Received 27 Jul 2011; revised 28 Aug 2011; accepted 31 Aug 2011; published 23 Sep 2011

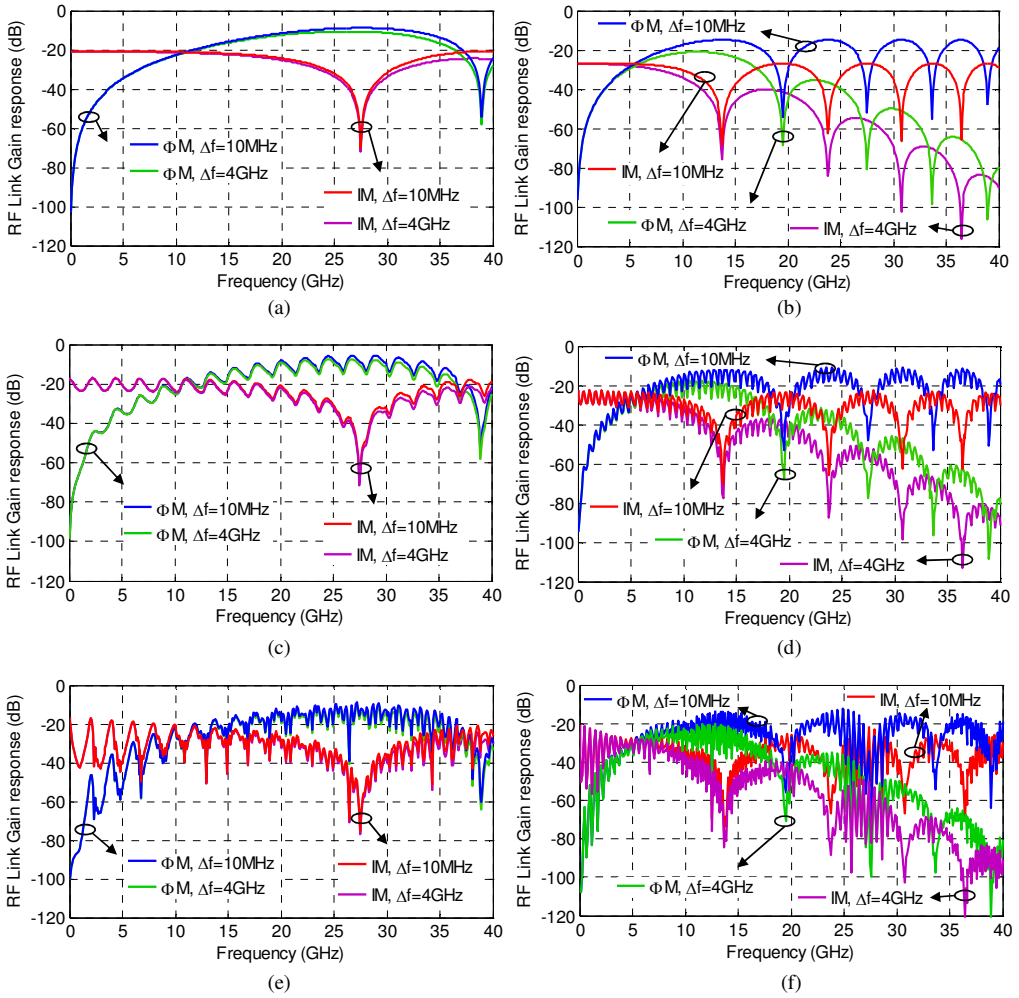

Fig. 7. G_{RF} response in a dispersive link for intensity (IM) and phase (ΦM) modulation with direct detection. (a) 5 km SMF. (b) 20 km SMF. (c) 5 km MMF and (d) 20 km MMF with central launching. (e) 5 km MMF and (f) 20 km MMF with uniform launching.

Finally, we will analyze the transversal filtering effect [17] that intrinsically characterizes the multimode propagation for different intensity launch conditions. Figure 7 (c) and (d) correspond to a selective central assignment of the light injection coefficient C_{mm} where the low-order mode groups have been excited following a Gaussian distribution, while Fig. 7 (e) and (f) refer to a uniform overfilled launch (OFL) condition. The comparison between both injection techniques corroborates that central launching results into a reduction in the depth of the transversal filtering notches as a consequence of forcing less intermodal dispersion. In this case, most of the energy is concentrated in the axial core region what subsequently reduces the effect of modal dispersion from the coupling of the high-order modes to the lower ones.

If a notch filter is introduced in order to suppress the red-shifted frequency sideband of the modulating signal prior to photodetection, CSE is expected to be completely avoided, as it actually occurs for Single Sideband Modulation links. Indeed, the application of our model to the case when the lower-frequency modulating band is attenuated by more than 38 dB, (FBG_A), results in a complete reduction of the typical CSE notches for both modulation choices. This behavior is displayed in Fig. 8 (a) for the SMF link and in Fig. 8 (b) for the MMF link with central launching, showing a comparison between the cases of maximum,

#151909 - $15.00 USD Received 27 Jul 2011; revised 28 Aug 2011; accepted 31 Aug 2011; published 23 Sep 2011

FBG_A, and minimum, FBG_B, attenuation. We can also observe how a reduction in the level of red-shifted frequency sideband suppression implies a minor CSE compensation (FBG_B). Note that the deep notch experienced in the baseband region for IM and in the vicinity of 5 GHz for ΦM is not actually related to the CSE, but to the fact that the optical carrier falls also into the notch of the FBG response when the electrical frequency is located into those regions.

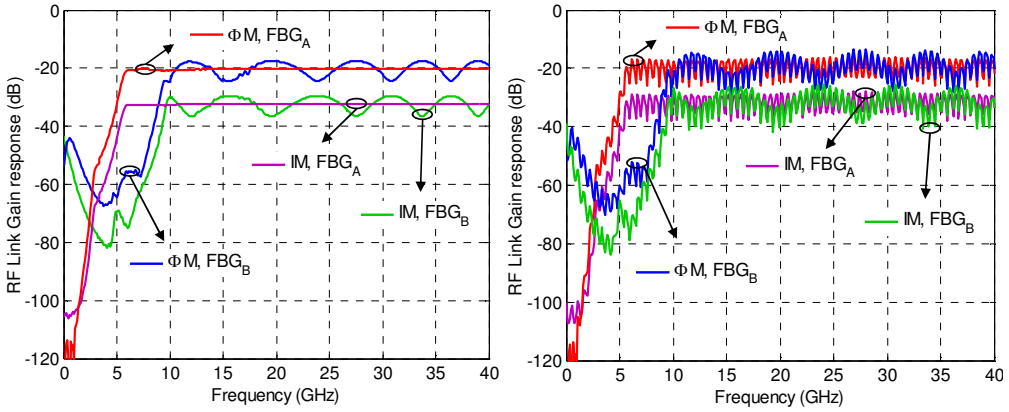

Fig. 8. G_{RF} response in a link comprising a dispersive fiber and a FBG notch filter comparing different sideband suppression levels (FBG_A and FBG_B), for intensity (IM) and phase (ΦM) modulation with direct detection. (a) 20 km SMF. (b) 20 km MMF with central launching.

The usefulness of our model becomes even clearer when the performance evaluation of filtered MWP links requires the analysis of the nonlinear distortion. In this context, Fig. 9 illustrates the analysis of the RF photodetected power for the modulating signal at Ω_1, (from $P_{RF}|_{out}(\Omega_1)$ in Eq. (7) and (26)), the IMD_2 term at Ω_1–Ω_2, (from $P_{RF}|_{out}(\Omega_1$–$\Omega_2)$ in Eq. (15) and (34)), and the IMD_3 term at $2\Omega_1$–Ω_2, (from $P_{RF}|_{out}(2\Omega_1$–$\Omega_2)$ in Eq. (18) and (37)), versus the RF modulator input power when the filtered MWP link consists of a 20 km SMF link and a FBG applying maximum suppression level (case FBG_A). The results computed for intensity modulation are plotted in solid lines while the ones obtained for phase modulation are plotted in dashed lines. Here a low-linewidth laser characterized by Δf = 10 MHz has been assumed. Apart from the predicted output level increase when ΦM is applied, we can appreciate that the computed OIP_2 and OIP_3 are respectively around 7 and 4 dB higher than for IM, again in complete agreement with [5]. For the computation of the total output noise spectral density N_{tot} , apart from the output contribution due to thermal noise at the input and thermal noise at the output for T = 290 K and the contribution of shot noise, we have assumed RIN_{laser} = −160 dBm/Hz, obtaining similar dynamic range figures for both modulation schemes: $SFDR_2$ = 81,75 dB·$Hz^{1/2}$ and $SFDR_3$ = 110,57 dB·$Hz^{2/3}$ for intensity modulation, while $SFDR_2$ = 83,12 dB·$Hz^{1/2}$ and $SFDR_3$ = 110,26 dB·$Hz^{2/3}$ for phase modulation.

#151909 - $15.00 USD Received 27 Jul 2011; revised 28 Aug 2011; accepted 31 Aug 2011; published 23 Sep 2011

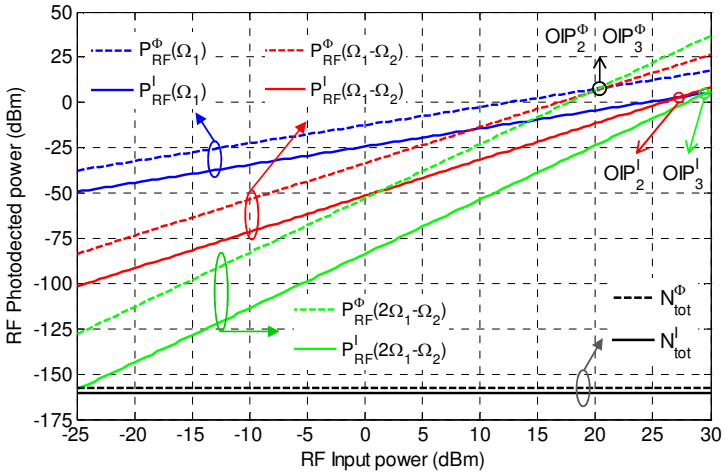

Fig. 9. RF photodetected power for the signal, IMD_2 and IMD_3 terms and output noise level as function of the input RF power for a link comprising a dispersive 20 km SMF and a FBG notch filter (maximum attenuation: FBG_A) when employing a low-linewidth laser, $\Delta f = 10$ MHz.

5. Conclusions

We have developed a general analytical propagation model for externally modulated *filtered MWP links*, a novel concept in which the effect of all intermediate optical components can be lumped into an optical transfer function $H(\omega)$ connecting the input to the output of the microwave system. The principal advantage of our model relies on the global character of the described filtered MWP link as it works under very general conditions for the coherence properties of the optical source and allows the analysis of both intensity and/or phase modulation techniques. This approach provides also the expressions leading to the computation of the main figures of merit, RF link gain, noise figure and spurious free dynamic range, enabling in consequence the performance evaluation of a wide range of complex MWP systems.

As a proof of principle, we have particularized the derived closed-form expressions to different well-known examples widely employed by the MWP community leading to a coincidence between the figures of merit formulas provided by this paper with those previously reported in the literature. With the purpose of illustrating the applicability of our model we have also computed the performance metrics of a non-standard radio over fiber system. The extension of the term *filtered MWP links* is envisaged to cover also a variety of fields including non-linear characterization of both amplitude and group delay ripples in chirped FBGs applied to microwave photonic filters, the design of complimentary optical filters in frequency discrimination systems for dynamic range optimization as well as multiport WDM optical distribution networks.

Acknowledgments

The authors wish to acknowledge the financial support given by the Research Excellency Award Program GVA PROMETEO 2008/092.

#151909 - $15.00 USD Received 27 Jul 2011; revised 28 Aug 2011; accepted 31 Aug 2011; published 23 Sep 2011